



Comparison of vertically aligned carbon nanotube array intercalated production among vermiculites in fixed and fluidized bed reactors

Qiang Zhang, Meng-Qiang Zhao, Jia-Qi Huang, Fei Wei *

Beijing Key Laboratory of Green Chemical Reaction Engineering and Technology, Department of Chemical Engineering, Tsinghua University, Beijing 100084, China

article info

Article history:

Received 28 August 2009

Received in revised form 14 November 2009

Accepted 28 November 2009

Available online 4 December 2009

Keywords:

Carbon nanotube arrays

Fluidization

Nanostructure

Powder technology

Chemical vapor deposition

abstract

Vertically aligned carbon nanotube (CNT) arrays with ordered nanostructure and extraordinary performance have become an important advanced material. CNTs were synchronously grown with high density to form aligned morphology, while the fine agglomerated structure was sensitive to the packing style of catalyst particles. Thus, synthesis of CNT arrays in a fixed bed or fluidized bed is an important issue. We reported that CNT arrays were grown from ethylene on a lamellar catalyst in a fixed bed reactor and a fluidized bed reactor, respectively. The reactor style affected the intercalated growth of CNT arrays greatly. The qualities of CNT array products in the fixed bed showed a distribution along the axis direction. The CNT arrays obtained at the top of the fixed bed were of good alignment and small diameter; while for the products obtained at the bottom of the reactor, CNT array blocks with higher densities, larger diameter, shorter length, and more defects, were formed. When CNT arrays were grown in a fluidized bed, they were of homogeneous structure, low densities, small uniform diameter, and had little defects, which can be attributed to available space, uniform temperature and reactant distribution in the fluidized bed reactor. These favored the mass production of CNT arrays with uniform properties in a fluidized bed reactor.

© 2009 Elsevier B.V. All rights reserved.

1. Introduction

Carbon nanotube (CNT) is an attractive material because of many unique properties originating from the small size, cylindrical structure, and large aspect ratio. CNTs have extremely high tensile strength (≈ 150 GPa), high modulus (≈ 1 TPa), and high thermal and electrical conductivity. They have found applications in composites, lithium-ion secondary battery, supercapacitor, field emission display, catalysis, inks, and transparent conductive film. It is found that the performance of CNTs strongly depends on the CNT agglomerated state [1,2]. For example, CNTs randomly entangle with each other when they cluster into CNT agglomerates [3], while they are orderly aligned with each other when forming CNT arrays [4–6]. The CNT agglomerates can be easily mass produced on metal active phases loading on porous particles [7–9]. The growth and applications of CNT agglomerates were widely investigated by many groups previously [9–15]. Several pilots mass production of agglomerated CNTs were realized in fluidized bed reactors [7–9]. However, the CNTs in the agglomerates are strongly entangled with each other. This hinders the dispersion of CNTs into isolated state. Furthermore, the length of CNTs in the agglomerated CNTs is hard to determine. CNTs are always shortened during the purification and further dispersion process [16]. While in vertically aligned CNT (VACNT) arrays, in which CNTs have a length

almost equal to that of the arrays (1–10,000 μm), are advantages of large aspect ratio, good orientation, and high purity. Compared with CNTs in the agglomerate form, it is much easier for VACNTs in array form to be de-bundled as fluffy CNTs [17]. Therefore, significant improvements in the electronic, mechanical, and thermal properties of polymer-VACNT composites have been achieved [1]. The ordered structure of VACNT array also brings novel applications, such as anisotropic conductive materials, membrane filtration materials, filaments, energy absorbing hybrid, and super elastic foams [18–21]. To our knowledge, VACNT array shows best performance for the applications mentioned above. Thus, mass production of VACNT array is needed.

Catalytic chemical vapor deposition (CVD) is the only method for the synthesis of VACNT array. The popular synthesis procedure is synthesizing VACNT array on flat substrate (wafer, quartz plate, MgO single crystal) in a fixed bed [4,5,22]. The productivity is small (b 1 g/h) because the surface area of the flat substrate is very limited (b 0.05 m^2/g). Moreover, due to the anisotropic morphology of a flat substrate, the substrate is difficult to be suspended or be moved. Thus, only a fixed bed with 1–10 pieces of substrates can be used for array growth in previous studies [4,5,23]. If CNT arrays can grow on a particle with a size of 1–1000 μm , then they can be easily operated using powder technology. Thus, various particles with large surface area, including spheres [24], fibers [25], and lamellar particles [19,26], have been used as substrates for the growth of VACNTs. Not only the productivity increases significantly, but also these particles are easily delivered in the reactor. Furthermore, if the size of lamellar particles,

* Corresponding author. Tel.: + 86 10 62785464; fax: + 86 10 62772051.

E-mail address: wf-dce@tsinghua.edu.cn (F. Wei).

such as vermiculite can be controlled to range from 10–200 μm , the VACNT arrays can be mass produced in a fluidized bed reactor [27].

Obviously, the reactor style affects the growth of CNTs greatly. For example, See et al. found the carbon yields obtained in fixed and fluidized bed reactors for agglomerated CNTs in the literature were consistent, but the fluidized bed reactors had the advantage of being able to accommodate a greater quantity of catalyst and therefore higher throughputs were achievable [28]. Qian et al reported growth of agglomerated multi-walled CNTs on porous $\text{Fe}/\text{Al}_2\text{O}_3$ catalyst both in fixed (packed) and fluidized bed reactors [29]. They found that significant changes in the bulk density and particle size of the CNT agglomerates were observed in the packed-bed reactor, while the fluidized bed reactor can perform well even after the volume and yield of CNTs are 6–7 times of that in the fixed bed reactor [29]. Recently, many groups have successfully mass produced agglomerated CNTs via a fluidized bed CVD [3,30–40]. While for the synthesis of VACNT array, the growth behavior of arrays is quite different from that of CNT agglomerates [7–9]. In previous studies, most CNT arrays were synthesized in a fixed bed – one piece of wafer or quartz plate with a diameter of 1–100 mm was put into a quartz tube (with a diameter of 3–100 mm and a length of 300–1500 mm). Thus, VACNT arrays can grow freely in the reactor, but the efficiency of the reactor was quite low. Growth of VACNT arrays in a fixed bed with high solid fraction is few mentioned in literature. But it is quite an important issue to realize the mass production of VACNT arrays.

To further understand the growth behavior of VACNT array, we demonstrated a comparison of VACNT array production in fixed and fluidized bed reactors using the same $\text{Fe}/\text{Mo}/\text{vermiculite}$ catalyst. The vermiculite is weathered micas in which the K^+ ions between the molecular sheets are replaced by Mg^{2+} and Fe^{2+} cations [41]. It is a kind of cheap natural resource, and can be used as the catalyst for the synthesis of VACNT arrays. The size of $\text{Fe}/\text{Mo}/\text{vermiculite}$ can be easily modulated, and its surface area is much larger than that of wafer or quartz plate. We have carried out the CVD growth of VACNT arrays on the novel $\text{Fe}/\text{Mo}/\text{vermiculite}$ catalyst both in fixed and fluidized bed reactors. With characterization by scanning electron microscope (SEM), transmission electron microscope (TEM), Raman spectra, and thermal gravimetric analysis (TGA), the growth behavior of VACNT arrays among vermiculite was fully illustrated. The effect of reactor style was also investigated, which is important for chemical engineers to scale up the process.

2. Experimental

2.1. Catalyst preparation

Vermiculite powder with a size of 100–300 μm and a bulk density of about 160 kg/m^3 was mined in Lingshou, Hebei Province of China. 20.0 g of vermiculites was exfoliated at 900 $^\circ\text{C}$ for 1 min. Then it was cooled down to room temperature, and was suspended in 200 mL distilled water to form a uniform suspension through strong stirring at 80 $^\circ\text{C}$. Subsequently, a solution of $\text{Fe}(\text{NO}_3)_3 \cdot 9\text{H}_2\text{O}$ and $(\text{NH}_4)_6\text{Mo}_7\text{O}_{24} \cdot 4\text{H}_2\text{O}$ was added slowly into the suspension. The mass ratio of the $\text{Fe}:\text{Mo}:\text{vermiculite}$ was 5:5:90. After soaking for 24 h, the exchangeable ion among the layers of vermiculite, such as Ca^{2+} , Mg^{2+} , K^+ , can be replaced by Fe^{3+} . Meanwhile, the lamellar structure was well preserved. Then the solution was filtrated, and the as obtained filtrated cake was further dried at 110 $^\circ\text{C}$ for 12 h. After further calcination at 400 $^\circ\text{C}$ for 1.0 h, a lamellar $\text{Fe}/\text{Mo}/\text{vermiculite}$ catalyst for VACNT array production was obtained.

2.2. VACNT array synthesis

The VACNT arrays were synthesized in a reactor operated in a fixed or a fluidized bed. The main body of the reactor was made of quartz glass with an inner diameter of 25 mm and a height of 700 mm. There

was a sintered porous plate used as the gas distributor at the bottom of the reactor. About 1.5 g $\text{Fe}/\text{Mo}/\text{vermiculite}$ catalyst was fed into the reactor before reaction. The height of initial $\text{Fe}/\text{Mo}/\text{vermiculite}$ catalyst was about 1.9 cm.

For fixed bed operation, the gases were fed from the top and passed through the catalyst particles. The reactor was heated to 650 $^\circ\text{C}$ in Ar atmosphere at a flow rate of 500 ml/min. Then 50 ml/min H_2 was introduced into the reactor for 10 min to reduce the catalyst. After reduction, 100 ml/min C_2H_4 serving as carbon source was introduced into the reactor for VACNT array growth. The growth time was controlled for 1.0 h and the height of as-grown CNTs were about 7.5 cm. The as-grown products were collected and divided into several parts according to its axis and radial distribution in the reactor. To investigate the qualities of the products grown at different positions in the fixed bed reactor, the products were gradually collected by a chemical spoon with a long affixed dipper. The products were sorted into several parts according to the axis and radial position in the reactor.

While for the fluidized bed operation, the gas mixture containing the carbon source reactant enters the bottom vessel of the reactor and then passes through the gas distributor, the fluidized bed units, and finally flows out into the atmosphere. The quartz fluidized bed reactor, mounted in an electrical tube furnace, was first heated to 650 $^\circ\text{C}$ in Ar atmosphere at a flow rate of 500 ml/min. Then 50 ml/min H_2 was added into the carrier gas for catalyst reduction for 10 min. In the fluidized bed operation, the catalysts were pushed apart from one another by the upflow of the gas at a sufficient velocity to cause mobility. When a mixture of $\text{C}_2\text{H}_4/\text{H}_2$ (100/50 ml/min) was introduced into the fluidized bed, VACNT arrays were grown among the vermiculite catalysts. After growth for 1.0 h, the reactor was cooled at Ar atmosphere. The carbon product was collected and characterized as follows.

2.3. Characterizations

The morphology of the VACNT array was characterized using a JSM 7401F SEM operated at 5.0 kV, and a JEM 2010 TEM operated at 120.0 kV. The sample for the TEM observation was prepared using a common sonication method. TGA (Perkin Elmer TGA 2050) was carried out to measure the amount of carbon deposited and to evaluate the purity of as-produced CNTs. The TGA analysis was conducted under an air atmosphere with a heating rate of 20 $^\circ\text{C}/\text{min}$ ramp between 30 and 900 $^\circ\text{C}$. Micro-Raman spectroscopy was performed on a Raman spectrometer (Renishaw, RM2000) equipped with a charged coupled device detector and an optical microscope for focusing the incident laser beam (a He–Ne laser excitation, 632.8 nm) to a 1–2 μm spot size.

3. Results and discussion

3.1. VACNT arrays grown in a fixed bed reactor

1.5 g $\text{Fe}/\text{Mo}/\text{vermiculite}$ catalyst was laid into a fixed bed reactor for the growth of VACNTs. The specific surface area of the exfoliated vermiculite was $8.0 \times 10^4 \text{ cm}^2/\text{g}$, which was equal to 10^4 1-in. wafer (the specific surface area of wafer was estimated to be $8.0 \text{ cm}^2/\text{g}$). Compared with previous wafer scale growth [4,5,22,23], the packing density of the catalyst was much higher. The $\text{Fe}/\text{Mo}/\text{vermiculite}$ catalysts were packed closely in the fixed bed. After reduction, C_2H_4 was introduced into the reactor and it decomposed into H_2 and CNTs. During the CVD process, the CNT arrays were grown among the vermiculite layers, leading to the expansion of catalyst particles. Thus, both the height and density of the fixed bed increased. The typical morphologies of the as-grown products at different positions in the fixed bed reactor were shown in Fig. 1. VACNT arrays, not CNT agglomerates, were synthesized among vermiculites. This was mainly

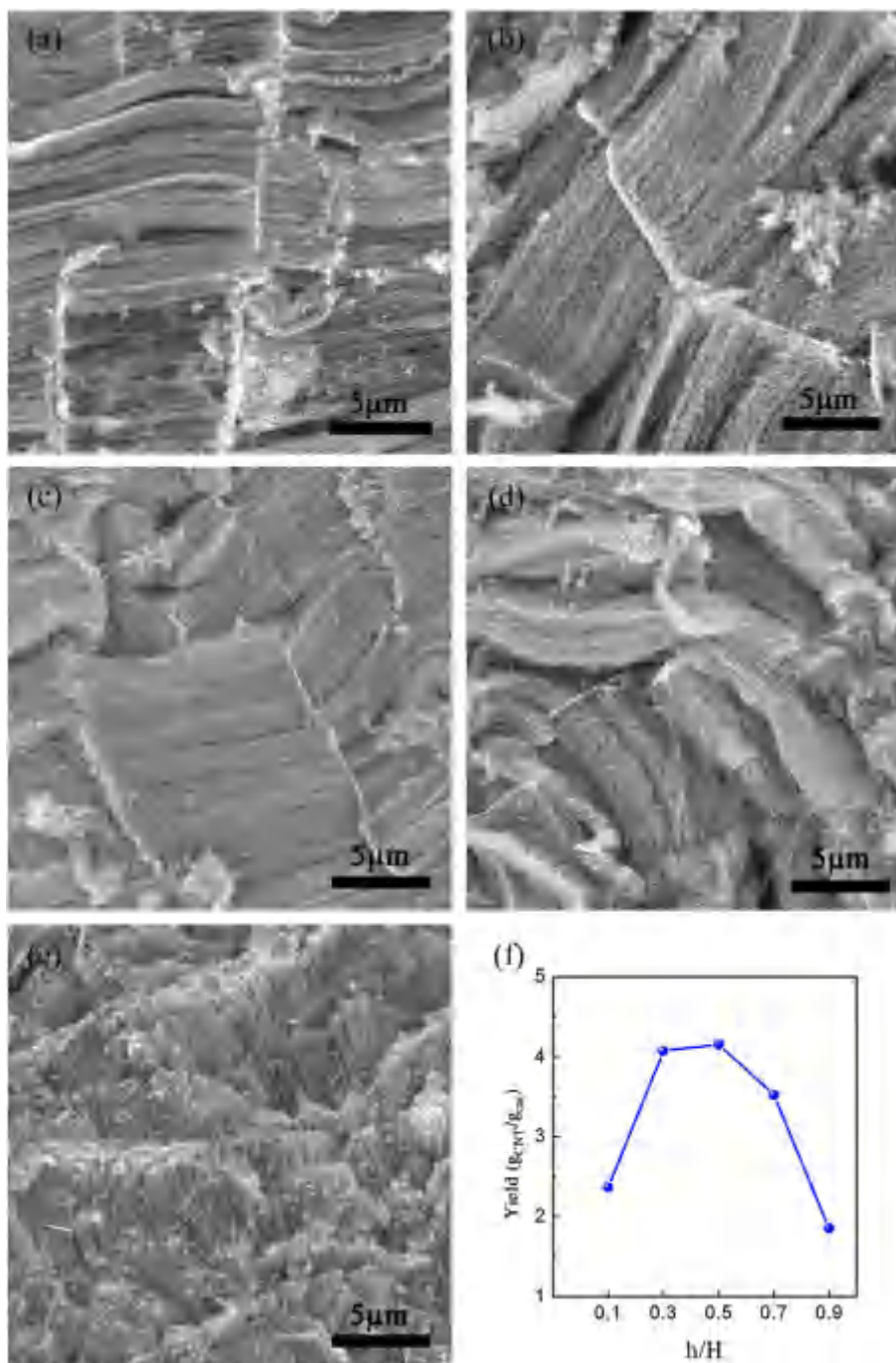


Fig. 1. Morphologies of VACNT array grown in a fixed bed reactor at different positions along the axis direction: h/H is (a) 0.1, (b) 0.3, (c) 0.5, (d) 0.7, and (e) 0.9, respectively; (f) the yield distribution of VACNT array at different positions.

attributed to the synchronous growth of CNTs among the vermiculite layers [42].

When using Fe/Mo/vermiculite as the catalyst in the fixed bed reactor, aligned CNT arrays intercalatedly grew among the vermiculites (Fig. 1). However, the carbon yield, diameter, and length of CNTs grown at various zones of the reactor were quite different. To quantitatively characterize the as-grown products, we defined the product at the position h/H , in which h is the distance from the top surface of the product's layer, and H is the height of the product's layer. At the top, the concentration of carbon source was high, while that of H_2 was low. The as-grown products were highly aligned CNT arrays intercalated among the lamellar catalyst (Fig. 1a). The length of VACNT was about 8.0–10.2 μm. The VACNT arrays grown on different

vermiculite layers still showed good alignment, although some vermiculite layers had been cracked into small pieces (the diameter of cracked vermiculite flakes ranged from 5 to 100 μm). When h increases, the concentration of carbon source decreased (the calculated concentration of C_2H_4 were decreased from 1.78 to 0.61 mol/m³ when h/H increased from 0.1 to 0.7), while that of H_2 increased. Thus the catalyst particles were reduced into metal particles more easily. Then more VACNT arrays can be obtained with high active catalyst and the carbon yield increased accordingly (Fig. 1f). The CNTs grown among lamellar catalyst showed good orientation, however, the as-grown bundles of VACNT arrays became crowded and some arrays began to bend (Fig. 1b–d). The diameter of vermiculite layers among CNT arrays was crushed into 2 to 8 μm at the

position h/H of 0.7 (Fig. 1d). At the bottom of the reactor, the density of the as-grown product was the highest. As demonstrated in Fig. 1e, the CNTs heavily crowded with each other. The layers of the lamellar substrate were curved, and the orientation among bundles of CNTs turned bad. This is because that expansion space was limited in the fixed bed. There was large stress among catalyst particles, which strongly limited the synchronous growth of VACNT array [42,43]. This effect was much clearer at the bottom of the fixed bed (Fig. 1e). Meanwhile, the length of CNT arrays was almost less than $5\ \mu\text{m}$, and the yield of CNT array decreased (Fig. 1f). Thus, it can be concluded that due to the limited growth space in the fixed bed, the alignment and length of as-grown CNT arrays decreased along the axis direction.

To further characterize the as-grown products in the fixed bed, TEM images were used to illustrate the fine structure. From the typical TEM image of the as-grown products shown in Fig. 2, at the top of the fixed bed, small diameter CNTs with an inner diameter of 3–5 nm and outer diameter of 9–15 nm, were grown among the lamellar catalyst (Fig. 2a). The CNTs showed good graphitization and high purity, and the wall number was about 5–20 (Fig. 2b). Little other impurities, including carbon spheres, carbon onions, or amorphous carbon, can be found. For the as-grown products at the bottom of fixed bed, thicker walled CNTs with a diameter of about 25 nm were also grown on the vermiculite catalyst (Fig. 2c). The diameter of CNTs increased obviously. Meanwhile, the graphite layer of CNTs became heavily distorted, indicating more defects were distributed in CNTs (Fig. 2d). They can be further confirmed by the Raman spectra. Typical multi-walled CNTs Raman spectra can be obtained with two typical peaks – G band at $1582\ \text{cm}^{-1}$ (E_{2g} graphite mode) and D band at $1350\ \text{cm}^{-1}$ (the defect mode). The intensity ratio of D band and G band (I_D/I_G) is positively related to the defect density in the CNT sample [24,25]. The I_D/I_G values of sample collected at different position of the reactor are shown in Fig. 3. The ratio

increased from 1.41 to 1.76 along the axis directions, indicating that the defect densities increased obviously, which consisted well with the TEM results shown in Fig. 2. We also examined the defect densities of the sample along the radial direction (at h/H is 0.9) by the ratio of D peak to G peak. As shown in Fig. 4b, the I_D/I_G values almost kept constant with increasing r/R , indicating the products at the radial direction were uniform. The results indicated that differences of products were mainly distributed along the axis direction, and the piston flow assumption was reasonable to describe the growth of VACNT array in a fixed bed reactor.

3.2. VACNT arrays grown in a fluidized bed reactor

The Fe/Mo/vermiculite catalysts were also laid into a fluidized bed reactor for the growth of VACNT arrays. The sizes of both the catalyst particles and as-grown products were 100–500 μm . They can be classified into A particles according to Geldart particle classification and show good fluidization behavior [44]. Here, the gas velocity was kept as 7.5 cm/s and the flow regime was bubbling fluidization. In the fluidized bed, particles were moving in the reactor. There were collisions among particles, or particles and bubbles. However, the lamellar structure of the vermiculite avoided the direct collisions among VACNT arrays. Furthermore, the obtained alternate CNT and vermiculite layers have good damping performance. They can withstand high cushioning with well morphology preservation [19]. Thus the VACNT arrays can still synchronously grow among the vermiculite layers. As demonstrated in Fig. 4, after a 1.0 h growth, highly aligned CNTs in array form were grown among the vermiculites. The arrays pushed the layers uniformly and the tortuosity factor of the as-grown CNTs was just about 1.15 ± 0.08 . The length of array was about 5.0–7.0 μm . The TEM images indicated that the as-grown products were in high purities (Fig. 4c). Multi-walled CNTs with an

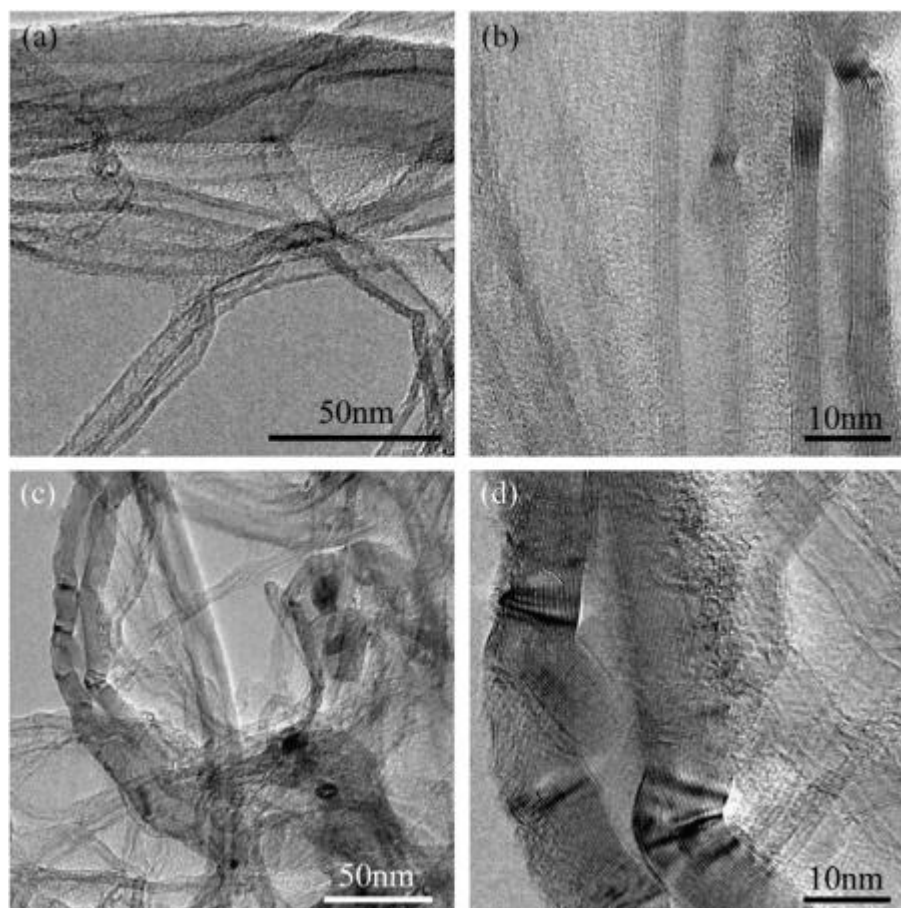


Fig. 2. TEM and high resolution TEM image of VACNT array grown in a fixed bed reactor: h/H is 0.1 (a and b) and 0.9 (c and d), respectively.

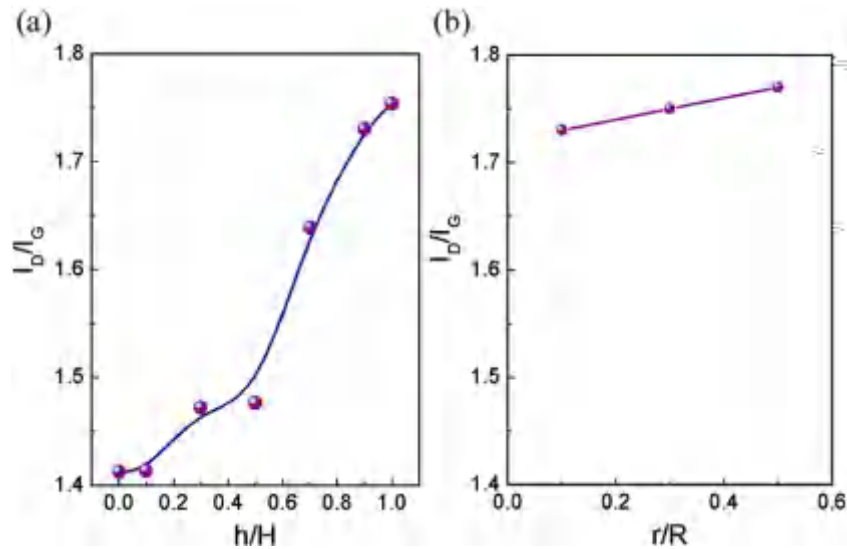


Fig. 3. The intensity ratio of D band to G band (I_D/I_G) in Raman spectra of VACNT products obtained at different zones in the fixed bed reactor; (a) is the axis distribution of I_D/I_G at the center line; (b) is the radial distribution of I_D/I_G at h/H of 0.9.

inner diameter of 3–5 nm, outer diameter of 6–10 nm, wall number of about 4–18, were grown. A few defects were demonstrated in the HRTEM images; however, the wall of the product was clean (Fig. 4d). The ratio of D peak to G peak in the Raman spectra was just 0.90, indicating the obvious lower defect density compared with that of products obtained from the fixed bed. The space time yield of the CNT array grown in the fluidized bed was $3.8 \text{ g}_{\text{CNT}}/\text{g}_{\text{cat}} \cdot \text{h}$ in the present study.

3.3. Comparison of VACNT array growth in fixed and fluidized bed reactors

VACNT arrays were successfully synthesized in fixed and fluidized bed reactors. The properties of the as-grown products are summarized in Table 1. The as-grown VACNT arrays in a fixed bed were inhomogeneous: the VACNT arrays at the top have longer length, smaller diameter, and lower defect density; while at the bottom of the

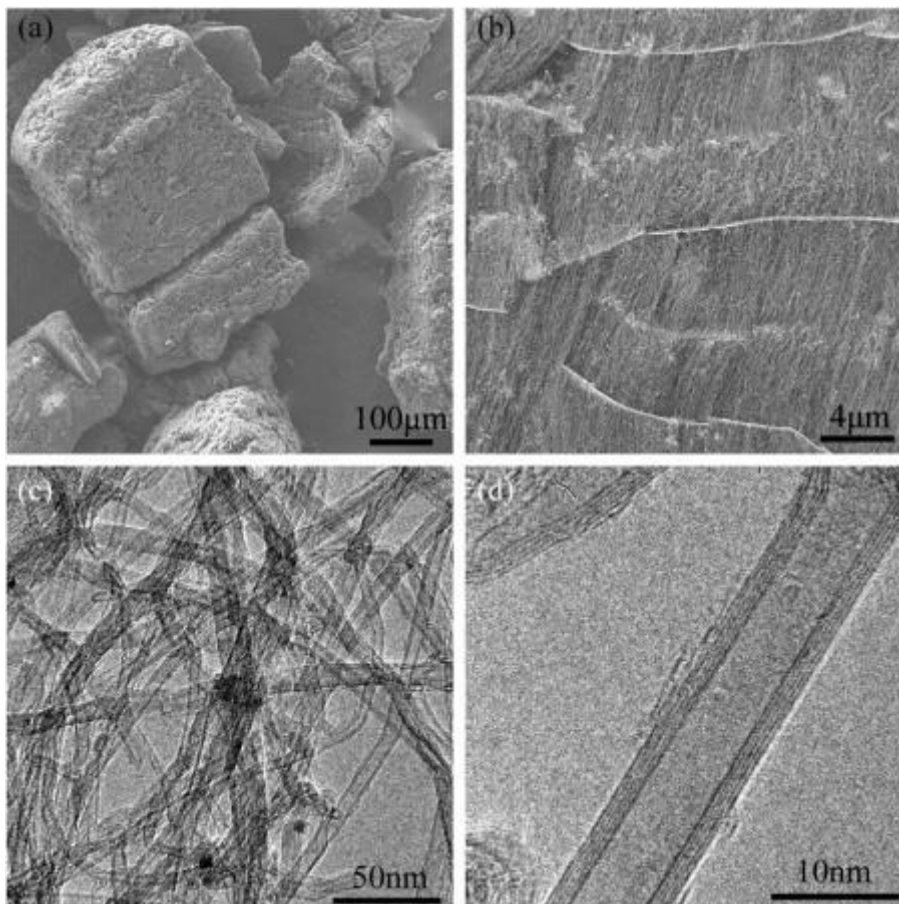


Fig. 4. SEM (a and b) and TEM (c and d) images of VACNT array grown in fluidized bed reactor.

Table 1
Comparison of the as-grown VACNT products grown among vermiculites in fixed and fluidized bed.

	Fixed bed 1 ^a	Fixed bed 2 ^a	Fluidized bed
Densities (g/L)	33.3	94.1	29.4
Space time yield ($g_{\text{CNT}}/g_{\text{cat}} \cdot h$) ^b	2.3	1.8	3.8
Length of the array (μm) ^c	8.0–10.2	3.0–5.0	5.0–7.0
Tortuosity factor ^d	1.16 ± 0.07	1.35 ± 0.10	1.15 ± 0.08
Outer diameter (nm) ^e	9–15	9–30	7–10
Inner diameter (nm) ^e	3–5	2.5–7	3–5
Wall number ^e	5–20	4–40	4–18
I_D/I_G ratio ^f	1.47	1.73	0.91

^a The product 1 from the fixed bed was at h/H of 0.3, while the product 2 from the fixed bed was at h/H of 0.9.

^b The space time yield of CNTs defined by the amount of VACNT arrays grown on per gram catalyst per hour, which was obtained by TGA.

^c The length was measured by SEM analysis.

^d The tortuosity factor of the CNTs, which is defined as the ratio of the length of the curved line between two points to the linear distance between the two points. It was obtained at a calculated scale of 5 μm .

^e The outer, inner diameter, and wall number of CNTs in the array were measured from the TEM images.

^f The I_D/I_G ratio was obtained from the Raman spectra.

reactor, the VACNT arrays have shorter length, larger diameter, and higher defect density. For the products produced in a fluidized bed, the products showed a homogenous structure: the tortuosity factor was small, the I_D/I_G value was low, and CNTs were straight; the diameter became uniform, and the defect density was small. This was mainly attributed to the relationship between the flow, mass transfer and reaction in the reactor. The C_2H_4 decomposed into H_2 and CNTs. The H_2 can reduce other catalyst particles. In the fixed bed, with h increasing, the concentration of carbon source decreased, and the concentration of H_2 increased, thus more catalyst will be reduced. During the CNT nucleation stage, if Fe nanoparticles were reduced fast, they were easily sintered on the vermiculites, leading to the formation of CNTs with large diameter at the bottom [24,45]. Meanwhile, with the growth of CNTs, the bed volume expanded. At the bottom, the space was limited, and the local stress was large due to the nature of packed solids expansion. Furthermore, less carbon source was provided. Discontinuous precipitation of CNTs took place, which resulted in the formation of CNTs with more defects. However, for the VACNT growth in the fluidized bed, it was with strong reactant mixing and good heat and mass transfer [7–9], leading to the uniform and easy catalyst nucleation. The carbon source diffused fast in the fluidized bed, leading to the uniform diameter of as-grown CNTs. Meanwhile, there was enough available space for VACNT array growth, thus the stress can be easily released, which gave rise to the formation of CNTs with good graphitization.

The above comparison of VACNT arrays produced in the two different kinds of reactors with the same catalyst indicates that the reactor style obviously affects the intercalated growth of CNT arrays among vermiculites. Due to the controlled hydrodynamics, available space, and efficient heat and mass transfer in the fluidized bed, large amount of VACNT arrays with controllable structure, uniform diameter, fewer defects, and stable macroscopic structure were obtained. Although the fluid dynamic is very complex in the fluidized bed, by careful catalyst design and parametric study, nanomaterials with an ordered structure can be well produced. This understanding is also important for developing mass production techniques for other powders with ordered nanostructure, such as aligned ZnO , ZnS , TiO_2 , Si , SnO_2 , and SiO_2 nanowire and nanotubes in the future.

4. Conclusions

The same lamellar Fe/Mo/vermiculite catalyst was used to study the difference between large scale growth of VACNT arrays in fixed and fluidized bed reactors. For the synthesis of high ordered VACNT

array, the qualities of the products strongly depended on the characteristics of reactors. For the VACNT grown in the fixed bed, the length, diameter, and alignment of CNTs in the array varied along the axis direction. While VACNT array with uniform diameter, length and few defects can be synthesized in the fluidized bed reactor at a large scale due to the high-efficiency flow and mass transfer. It can be found through the experimental comparison that the fluidized bed allows the controllable large scale synthesis of VACNT arrays with uniform properties, which also has great potential applications for mass production of high quality nanomaterials with ordered structure in future.

Acknowledgements

This study was supported by the Natural Science Foundation of China (No. 2007AA03Z346, No. 20736007) and the China National Program (No. 2006CB932702).

References

- [1] J.K.W. Sandler, J.E. Kirk, I.A. Kinloch, M.S.P. Shaffer, A.H. Windle, *Polymer* 44 (2003) 5893–5899.
- [2] D.S. Su, *ChemSusChem* 2 (2009) 1009–1020.
- [3] Y. Wang, F. Wei, G.H. Luo, H. Yu, G.S. Gu, *Chemical Physics Letters* 364 (2002) 568–572.
- [4] W.Z. Li, S.S. Xie, L.X. Qian, B.H. Chang, B.S. Zou, W.Y. Zhou, R.A. Zhao, G. Wang, *Science* 274 (1996) 1701–1703.
- [5] S.S. Fan, M.G. Chapline, N.R. Franklin, T.W. Tomblor, A.M. Cassell, H.J. Dai, *Science* 283 (1999) 512–514.
- [6] F. Wei, Q. Zhang, W.Z. Qian, G.H. Xu, R. Xiang, Q. Wen, Y. Wang, G.H. Luo, *New Carbon Materials* 22 (2007) 271–282.
- [7] C.H. See, A.T. Harris, *Industrial & Engineering Chemistry Research* 46 (2007) 997–1012.
- [8] R. Philippe, A. Morançais, M. Corrias, B. Caussat, Y. Kihn, P. Kalck, D. Plee, P. Gaillard, D. Bernard, P. Serp, *Chemical Vapor Deposition* 13 (2007) 447–457.
- [9] F. Wei, Q. Zhang, W.Z. Qian, H. Yu, Y. Wang, G.H. Luo, G.H. Xu, D.Z. Wang, *Powder Technology* 183 (2008) 10–20.
- [10] J. Zhang, X. Liu, R. Blume, A.H. Zhang, R. Schlogl, D.S. Su, *Science* 322 (2008) 73–77.
- [11] Y.J. Tian, H.X. Yang, Y.B. Cui, S.L. Zhan, Y.F. Chen, *Chemical Communications* (2008) 3299–3301.
- [12] Y.B. Cui, X.F. Wu, H. Wu, Y.J. Tian, Y.F. Chen, *Materials Letters* 62 (2008) 3878–3880.
- [13] D.S. Su, X.W. Chen, X. Liu, J.J. Delgado, R. Schlogl, A. Gajovic, *Advanced Materials* 20 (2008) 3597–3600.
- [14] R.T. Lv, S. Tsuge, X.C. Gui, K. Takai, F.Y. Kang, T. Enoki, J.Q. Wei, J.L. Gu, K.L. Wang, D. H. Wu, *Carbon* 47 (2009) 1141–1145.
- [15] F.C.C. Moura, R.M. Lago, *Applied Catalysis B-environmental* 90 (2009) 436–440.
- [16] P.X. Hou, C. Liu, H.M. Cheng, *Carbon* 46 (2008) 2003–2025.
- [17] Q. Zhang, G.H. Xu, J.Q. Huang, W.P. Zhou, M.Q. Zhao, Y. Wang, W.Z. Qian, F. Wei, *Carbon* 47 (2009) 538–541.
- [18] A.Y. Cao, P.L. Dickrell, W.G. Sawyer, M.N. Ghasemi-Nejhad, P.M. Ajayan, *Science* 310 (2005) 1307–1310.
- [19] Q. Zhang, M.Q. Zhao, Y. Liu, A.Y. Cao, W.Z. Qian, Y.F. Lu, F. Wei, *Advanced Materials* 21 (2009) 2876–2880.
- [20] K.L. Jiang, Q.Q. Li, S.S. Fan, *Nature* 419 (2002) 801–801.
- [21] Q.W. Li, Y. Li, X.F. Zhang, S.B. Chikkannanavar, Y.H. Zhao, A.M. Dangelewicz, L.X. Zheng, S.K. Doorn, Q.X. Jia, D.E. Peterson, P.N. Arendt, Y.T. Zhu, *Advanced Materials* 19 (2007) 3358–3363.
- [22] K. Hata, D.N. Futaba, K. Mizuno, T. Namai, M. Yumura, S. Iijima, *Science* 306 (2004) 1362–1364.
- [23] Y. Murakami, S. Chiashi, Y. Miyauchi, M.H. Hu, M. Ogura, T. Okubo, S. Maruyama, *Chemical Physics Letters* 385 (2004) 298–303.
- [24] Q. Zhang, J.Q. Huang, M.Q. Zhao, Y. Wang, W.Z. Qian, F. Wei, *Carbon* 46 (2008) 1152–1158.
- [25] Q. Zhang, W.Z. Qian, R. Xiang, Z. Yang, G.H. Luo, Y. Wang, F. Wei, *Materials Chemistry And Physics* 107 (2008) 317–321.
- [26] C.L. Pint, S.T. Pheasant, M. Pasquali, K.E. Coulter, H.K. Schmidt, R.H. Hauge, *Nano Letters* 8 (2008) 1879–1883.
- [27] Q. Zhang, M.Q. Zhao, J.Q. Huang, Y. Liu, Y. Wang, W.Z. Qian, F. Wei, *Carbon* 47 (2009) 2600–2610.
- [28] C.H. See, A.T. Harris, *Chemical Engineering Journal* 144 (2008) 267–269.
- [29] W.Z. Qian, F. Wei, Z.W. Wang, T. Liu, H. Yu, G.H. Luo, L. Xiang, X.Y. Deng, *AIChE Journal* 49 (2003) 619–625.
- [30] C.H. See, O.M. Dunens, K.J. MacKenzie, A.T. Harris, *Industrial & Engineering Chemistry Research* 47 (2008) 7686–7692.
- [31] D. Venegoni, P. Serp, R. Feurer, Y. Kihn, C. Vahlas, P. Kalck, *Carbon* 40 (2002) 1799–1807.
- [32] C.B. Xu, J. Zhu, *Nanotechnology* 15 (2004) 1671–1681.
- [33] A. Morançais, B. Caussat, Y. Kihn, P. Kalck, D. Plee, P. Gaillard, D. Bernard, P. Serp, *Carbon* 45 (2007) 624–635.

- [34] S.Y. Son, Y. Lee, S. Won, D.H. Lee, S.D. Kim, S.W. Sung, *Industrial & Engineering Chemistry Research* 47 (2008) 2166–2175.
- [35] C.T. Hsieh, Y.T. Lin, W.Y. Chen, J.L. Wei, *Powder Technology* 192 (2009) 16–22.
- [36] C.T. Hsieh, Y.T. Lin, J.Y. Lin, J.L. Wei, *Materials Chemistry And Physics* 114 (2009) 702–708.
- [37] Y.L. Li, I.A. Kinloch, M.S. Shaffer, J.F. Geng, B. Johnson, A.H. Windle, *Chemical Physics Letters* 384 (2004) 98–102.
- [38] Q. Zhang, H. Yu, Y. Liu, W.Z. Qian, Y. Wang, G.H. Luo, F. Wei, *Nano* 3 (2008) 45–50.
- [39] X.B. Liu, H. Sun, Y. Chen, R. Lau, Y.H. Yang, *Chemical Engineering Journal* 142 (2008) 331–336.
- [40] M. Bierdel, S. Buchholz, V. Michele, L. Mieczko, R. Rudolf, M. Voetz, A. Wolf, *Physica Status Solidi B-Basic Solid State Physics* 244 (2007) 3939–3943.
- [41] Y. El Mouzdahir, A. Elmchaouri, R. Mahboub, A. Gil, S.A. Korili, *Powder Technology* 189 (2009) 2–5.
- [42] Q. Zhang, W.P. Zhou, W.Z. Qian, R. Xiang, J.Q. Huang, D.Z. Wang, F. Wei, *Journal Of Physical Chemistry C* 111 (2007) 14638–14643.
- [43] E.R. Meshot, A.J. Hart, *Applied Physics Letters* 92 (2008) 113107.
- [44] D. Geldart, *Powder Technology* 7 (1973) 285–292.
- [45] Y. Liu, W.Z. Qian, Q. Zhang, G.Q. Ning, G.H. Luo, Y. Wang, D.Z. Wang, F. Wei, *Chemical Engineering & Technology* 32 (2009) 73–79.